NUMERICAL IMPLEMENTATION OF AN ORTHOTROPIC PLASTICITY MODEL IN THE ABAQUS FINITE ELEMENT CODE AND ASSOCIATED SIMULATIONS OF SHEET METAL FORMING TESTS

Luciano Pessanha Moreira
Universidade Federal Fluminense, Av. dos Trabalhadores 420 CEP 27 255-125 Volta Redonda RJ Brazil
luciano.moreira@metal.eeimvr.uff.br

Gérard Ferron
Laboratoire de Physique et Mécanique des Matériaux, Université de Metz, Ile du Saulcy 57045 Metz Cedex 01 France
ferron@lpmm.univ-metz.fr

Abstract. *In this work, the implementation procedures for the user Fortran subroutines of the commercial finite element code ABAQUS are described for the particular case of linear elasticity and a plasticity model proposed in the context of the flow theory along with the isotropic hardening assumption. The general elasto-plasticity 3D case is first presented and applied to the implicit and explicit techniques available in the ABAQUS FE code. Afterwards, th equations for the plane-stress case are presented for either procedures. The corresponding implementation procedures are applied to the plane-stress orthotropic plasticity model proposed by Ferron et al. [Int. J. Plast. 10 (1994) 431]. Finally, the implemented user subroutines are validated by means of numerical simulations of sheet-metal forming tests, namely, the hemispherical punch stretching and the cup-drawing, perfomed with the ABAQUS/Standard and ABAQUS/Explicit FE codes wherein the Hill's quadratic [Proc. of the Royal Society of London A193 (1948) 281] plasticity model is available. The comparison between the experimental results and the associated numerical predictions obtained with Ferron's plasticity model shows either the pertinent conditioning of the user subroutines regarding the number of increments and the computation cost time and the importance of an accurate description of the range of stresses states involved in sheet-metal forming processes.*

Keywords*: orthotropic plasticity, yield criterion, numerical simulation, finite element method, sheet-metal forming.*

1. Introduction

Sheet metal forming is an important manufacturing process widely used to produce complex stamped parts starting from flat blank sheets in sectors such as the automotive as well as food and beverage cans industries. Owing to the global economic context these sectors are urged to be extremely competitive by decreasing production costs and increasing the process efficiency. The numerical simulation combined with the sheet metal forming skill represents one of technological innovations adopted to achieve these requirements by decreasing the time and cost consuming traditional tryout steps. In the last 20 years, considerable efforts have been made to improve the finite element method (FEM) based upon incremental or one-step techniques for solving non-linear problems arising from material behavior, geometry and friction. Moreover, user-friendly graphical interfaces together with the increasing computer capacity also promoted the numerical simulation to analyze the sheet metal forming process in an industrial scale. In view of these advances, the questions arising from the accuracy or the limitations related to the type of material description adopted became particularly important. From this standpoint, a phenomenological approach is generally favored owing to its straightforward numerical implementation in finite element programs and low computation costs (CPU time) in comparison to physically motivated models based upon polycrystalline and combined approaches.

The present work aims at presenting the numerical procedures used together with the user material Fortran subroutines **UMAT** and **VUMAT** available respectively in the implicit and explicit versions of the commercial ABAQUS finite element (FE) code. First, the general 3D and plane-stress elasto-plasticity case are outlined for the generalized Hooke's law together with the associated plastic flow theory. Afterwards, the plane-stress orthotropic plasticity description proposed by Ferron et al. (1994), hereafter, Ferron's model, is initially recalled so as to explain the methods used to determine the coefficients defining the initial material anisotropy as well as to present its extension to the three-dimensional (3D). The equations needed for the implementation of Ferron's model in the ABAQUS FE code are then presented. Finally, the numerical predictions obtained with Ferron's model are compared to the experimental results obtained from sheet-metal forming tests, to be precise, the hemispherical punch stretching and the cup-drawing.

2. Numerical implementation of Ferron's model in the ABAQUS FE code

In this section, the procedures to implement the ABAQUS Fortran user material subroutines are presented for the particular case of the Hooke's isotropic elasticity law and a plasticity model based on the flow theory together with the isotropic work-hardening assumption. Firstly, the general 3D case for elasto-plasticity is outlined and applied to the implicit and explicit integration techniques available in the ABAQUS FE code by means of the user subroutines **UMAT** and **VUMAT** respectively. Then, the corresponding equations for the plane-stress case are developed. Finally, implementation procedures are applied to Ferron's model for the plane-stress and 3D cases.

2.1. General 3D case

2.1.1. Rate constitutive equations

Assuming first the assumption of small elastic strains, the elastoplastic behavior description is based upon the additive decomposition of the total strain-rate tensor into an elastic part and a plastic part, i.e.,

$$\dot{\boldsymbol{\varepsilon}} = \dot{\boldsymbol{\varepsilon}}^{\mathbf{e}} + \dot{\boldsymbol{\varepsilon}}^{\mathbf{p}} \tag{1}$$

In Eq. (1) the elastic behavior can be described by the Hooke's linear elasticity law :

$$\dot{\boldsymbol{\sigma}} = \mathbf{C}^{\mathbf{e}} : \dot{\boldsymbol{\varepsilon}}^{\mathbf{e}} = \mathbf{C}^{\mathbf{e}} : \left[\dot{\boldsymbol{\varepsilon}} - \dot{\boldsymbol{\varepsilon}}^{\mathbf{p}} \right] \tag{2}$$

where $\mathbf{C}^{\mathbf{e}}$ is the elasticity tensor and $\dot{\boldsymbol{\varepsilon}}^{\mathbf{e}}$ is the elastic strain-rate tensor. On the other hand, the plastic strain-rate tensor in Eq. (2) is defined by the plastic flow rule given by :

$$\dot{\boldsymbol{\varepsilon}}^{\mathbf{p}} = \dot{\lambda} \frac{\partial g}{\partial \boldsymbol{\sigma}} \tag{3}$$

associated to the yield function described under the isotropic work-hardening assumption by the following form :

$$f = F(\boldsymbol{\sigma}) - \overline{\sigma} \tag{4}$$

where $\boldsymbol{\sigma}$ is Cauchy stress tensor, $F(\boldsymbol{\sigma})$ is a first degree homogeneous stress function and $\overline{\sigma}$ is a scalar measure of the current effective stress. The plastic multiplier $\dot{\lambda}$ in Eq. (3) is defined by introducing first the equivalent plastic work principle, that is, $\boldsymbol{\sigma} : \dot{\boldsymbol{\varepsilon}}^{\mathbf{p}} = \overline{\sigma}\, \dot{\overline{\varepsilon}}^{\mathrm{p}}$, together with the associated flow rule (3) :

$$\boldsymbol{\sigma} : \dot{\lambda} \frac{\partial f}{\partial \boldsymbol{\sigma}} = \overline{\sigma}\, \dot{\overline{\varepsilon}}^{\mathrm{p}} \tag{5}$$

and then by employing the Euler's identity in the yield function (4) for the elasto-plastic loading condition, *i.e.*, $f = 0$:

$$F(\boldsymbol{\sigma}) = \overline{\sigma} = \boldsymbol{\sigma} \frac{\partial f}{\partial \boldsymbol{\sigma}} \tag{6}$$

resulting that the plastic multiplier $\dot{\lambda}$ is equal to the effective plastic strain-rate $\dot{\overline{\varepsilon}}^{\mathrm{p}}$ conjugated of the effective stress $\overline{\sigma}$. The elastoplastic behavior description is completed by defining the work-hardening evolution with the plastic strain relating the effective stress-rate to the effective strain-rate :

$$\dot{\overline{\sigma}} = H(\overline{\sigma})\, \dot{\overline{\varepsilon}}^{\mathrm{p}} \tag{7}$$

where $H(\overline{\sigma}) = \mathrm{d}\overline{\sigma} / \mathrm{d}\overline{\varepsilon}^{\mathrm{p}}$ is the work-hardening rate.

2.1.2. General integration method

The ABAQUS FE code provides at the beginning of each time step and for each element integration point, the stress tensor components $\boldsymbol{\sigma}$, the increments of the total strain tensor $\Delta\boldsymbol{\varepsilon}$ and all yield function internal variables. Bearing in mind deformation-driven problems, as is the case in displacement-based and mixed FE formulations, the stress state at the end of the time step is then obtained from the strain history by means of an integration algorithm of the rate constitutive equations in an incremental process. The general integration procedure is based upon an elastic predictor- plastic corrector algorithm commonly known as the return mapping algorithms. So as to abridge the notation, let us denote ξ^{t} as the current values of all variables at the beginning of the time step, ξ^{Trial} as the quantities referring to the elastic prediction and the corrected values at the end of the time step as $\xi^{\mathrm{t+\Delta t}}$. Therefore, the trial stress components are computed from an elastic prediction through the use of the Hooke's law (2) :

$$\sigma_{\mathrm{ij}}^{\mathrm{trial}} = \sigma_{\mathrm{ij}}^{\mathrm{t}} + C_{\mathrm{ijkl}}^{\mathrm{e}}\, \Delta\varepsilon_{\mathrm{kl}}^{\mathrm{e}} = \sigma_{\mathrm{ij}}^{\mathrm{t}} + C_{\mathrm{ijkl}}^{\mathrm{e}} \left[\Delta\varepsilon_{\mathrm{kl}} - \Delta\varepsilon_{\mathrm{kl}}^{\mathrm{p}} \right] \tag{8}$$

with $C_{\mathrm{ijkl}}^{\mathrm{e}} = \lambda\, \delta_{\mathrm{ij}}\delta_{\mathrm{kl}} + \mu\, (\delta_{\mathrm{ik}}\delta_{\mathrm{jl}} + \delta_{\mathrm{il}}\delta_{\mathrm{jk}})$ for the case of isotropic elasticity, where λ and μ are the Lame's coefficients. The elastoplastic loading occurs during the time step if the yield condition is violated by the trial state of stress, i.e., if :

$$F(\sigma_{\mathrm{ij}}^{\mathrm{trial}}) - \overline{\sigma}^{\,\mathrm{t}} \geq 0 \tag{9}$$

In that case, the new state of stress is then obtained from the plastic correction of the trial state of stress according to the user material subroutines **UMAT** and **VUMAT** available in the ABAQUS/Standard and Explicit FE codes respectively.

2.1.3. ABAQUS/Standard procedure (UMAT)

The numerical integration procedure used with **UMAT** is based upon the implicit backward Euler scheme whereas the solution of the constitutive equations is made with the Newton's method. Firstly, it is necessary to calculate the plastic corrections to the trial stress state given by Eq. (8). Then, the elastoplastic tangent operator must be determined. Let us denote $c(\xi)$ the correction to the variable ξ. From Hooke's law (2), the corrections associated to the stresses and plastic strain increments are related by :

$$c(\sigma_{ij}) = - C^{e}_{ijkl}\, c(\Delta\varepsilon^{p}_{kl}) \tag{10}$$

The effective stress-strain relationship, Eq. (7), must also be satisfied leading to the following Newton's equation :

$$c(\bar{\sigma}) = H(\bar{\sigma})\, c(\Delta\bar{\varepsilon}^{p}) + \Delta\bar{\varepsilon}^{p}\, \frac{\partial H(\bar{\sigma})}{\partial\bar{\sigma}}\, c(\bar{\sigma}) = \hat{H}(\bar{\sigma})\, c(\Delta\bar{\varepsilon}^{p}) \tag{11}$$

with

$$\hat{H}(\bar{\sigma}) = H(\bar{\sigma}) \Big/ \left[1 - \frac{\partial H(\bar{\sigma})}{\partial\bar{\sigma}}\, \Delta\bar{\varepsilon}^{p} \right] \tag{12}$$

The elasto-plastic loading condition, Eq. (4), is not satisfied exactly until the solution is reached, that is,

$$F_{,\,ij}\, c(\sigma_{ij}) - c(\bar{\sigma}) = - f \tag{13}$$

where $F_{,ij} = \partial F(\sigma_{ij}) \big/ \partial\sigma_{ij}$. Besides, the associated plastic flow rule, Eq. (3), also provides the following corrections :

$$c(\Delta\varepsilon^{p}_{ij}) - F_{,\,ij}\, c(\Delta\bar{\varepsilon}^{p}) - \Delta\bar{\varepsilon}^{p} F_{,\,ijkl}\, c(\sigma_{kl}) = F_{,\,ij}\, \Delta\bar{\varepsilon}^{p} - \Delta\varepsilon^{p}_{ij} \tag{14}$$

where $F_{,ijkl} = \partial^{2} F(\sigma_{ij}) \big/ \partial\sigma_{ij}\, \partial\sigma_{kl}$. By combining Eqs. (10-14), the following set of Newton's equations for the corrections upon the plastic strain components is obtained :

$$c(\Delta\varepsilon^{p}_{mn}) \left[\delta_{im}\delta_{jn} + C^{e}_{klmn} \left(F_{,ijkl}\, \Delta\bar{\varepsilon}^{p} + F_{,ij}\, F_{,kl} \Big/ \hat{H}(\bar{\sigma}) \right) \right] = F_{,ij} \left(\Delta\bar{\varepsilon}^{p} + f \Big/ \hat{H}(\bar{\sigma}) \right) - \Delta\varepsilon^{p}_{ij} \tag{15}$$

Once the $c(\Delta\varepsilon^{p}_{mn})$ values are calculated, the stress components at the end of the time step are obtained iteratively by correcting the trial stress state, Eq. (8), until the elasto-plastic loading condition is satisfied within a given accuracy :

$$\sigma_{ij}\Big|_{N} = \sigma_{ij}\Big|_{N-1} - C^{e}_{ijkl}\, c(\Delta\varepsilon^{p}_{kl})\Big|_{N} \tag{16}$$

where *N* is the current local Newton iteration. It should be noted that the correction in Eq. (16) is collinear with the plastic strain increment, and thus should be referred to as "normal return", the term "radial return" referring to the von Mises circle in the deviatoric stress plane.

The elastoplastic tangent operator is defined by consistent linearization of the response function resulting from the integration algorithm as proposed by Simo and Taylor (1985). The consistent stiffness matrix is then obtained by taking variations with respect to all variables. Firstly, the Hooke's law, Eq. (2), together with the total strain decomposition, Eq. (1), provide the variations between the strain and stress components :

$$\partial\varepsilon_{ij} = S^{e}_{ijkl}\, \partial\sigma_{ij} + \partial\varepsilon^{p}_{ij} \tag{17}$$

where S^{e}_{ijkl} is the elastic compliances tensor. Afterwards, the variations in the associated plastic flow rule, Eq. (3), the elastoplastic loading condition, Eq. (4), and the effective stress-strain relationship, Eq. (7), give, respectively :

$$\partial\varepsilon^{p}_{ij} = \partial\bar{\varepsilon}^{p}\, F_{,\,ij} + \Delta\bar{\varepsilon}^{p}\, F_{,\,ijkl}\, \partial\sigma_{kl} \tag{18}$$

$$F_{,\,ij}\, \partial\sigma_{ij} - \partial\bar{\sigma} = 0 \tag{19}$$

$$\partial\bar{\sigma} = H(\bar{\sigma})\, \partial\bar{\varepsilon}^{p} \tag{20}$$

By eliminating $\partial\bar{\sigma}$ and $\partial\bar{\varepsilon}^{p}$ in Eqs. (19) and (20) and replacing the resulting expression in Eq. (18), gives :

$$\partial\varepsilon^{p}_{ij} = F_{,\,ij}\, F_{,\,kl} \Big/ H(\bar{\sigma}) + \Delta\bar{\varepsilon}^{p}\, F_{,\,ijkl}\, \partial\sigma_{kl} \tag{21}$$

and then returning in Eq. (17), one obtains the following system of equations :

$$\partial\varepsilon_{ij} = S^{ep}_{ijkl}\, \partial\sigma_{kl} = \left[F_{,\,ij}\, F_{,\,kl} \Big/ H(\bar{\sigma}) + \Delta\bar{\varepsilon}^{p}\, F_{,\,ijkl} + S^{e}_{ijkl} \right] \partial\sigma_{kl} \tag{22}$$

Finally, the consistent elastoplastic tangent operator is obtained by inverting the elastoplastic compliances matrix, that is, $J^{t+\Delta t}_{ijkl} = (\partial\sigma_{ij} / \partial\varepsilon_{kl})^{t+\Delta t} = \left[S^{ep}_{ijkl} \right]^{-1}$.

2.1.4. ABAQUS/Explicit procedure (VUMAT)

In the Abaqus/Explicit code, the global equilibrium equations are solved by means of an explicit integration technique, which, in turn, does not require neither iterations nor the definition of the elastoplastic tangent operator. Thus, the integration of the constitutive equations is simply obtained from the plastic strain increments when the elastoplastic loading condition is verified. In this case, the state of stress at the end the time step is determined from the knowledge of the plastic strain increments, that is, by the correction of the trial stress state :

$$\sigma_{ij}^{t+\Delta t} = \sigma_{ij}^{trial} - 2\mu\,\Delta\varepsilon_{ij}^{p} \tag{23}$$

Since the plastic strain increments are known from the associated plastic flow rule, Eq. (3), the only quantity to be defined for obtaining the values of all variables at the end of the time step is thus the effective plastic strain increment. An appropriate procedure for determining the effective plastic strain increment consists of calculating the plastic work associated to the time step increment :

$$\sigma_{ij}^{t+\Delta t}\,\Delta\varepsilon_{ij}^{p} = \overline{\sigma}^{t+\Delta t}\,\Delta\overline{\varepsilon}^{p} \tag{24}$$

Using Eqs. (3) and (7), $\Delta\varepsilon_{ij}^{p} = \Delta\overline{\varepsilon}^{p}\,F_{,ij}^{trial}$ and $\overline{\sigma}^{t+\Delta t} = \overline{\sigma}^{t} + H(\overline{\sigma})^{t}\,\Delta\overline{\varepsilon}^{p}$, with Eq. (23) and replacing in Eq. (24) :

$$\Delta\overline{\varepsilon}^{p} = \frac{(\sigma_{ij}\,F_{,ij})^{trial} - \overline{\sigma}^{\,t}}{H(\overline{\sigma})^{t} + 2\mu\,(F_{,ij}\,F_{,ij})^{trial}} \tag{25}$$

where the terms $(\cdot)^{trial}$ are calculated for the trial stress state of stress and $(\sigma_{ij}\,F_{,ij})^{trial} = F(\sigma_{ij}^{trial})$ according to Eq. (6).

2.2. Plane-stress case

In the plane-stress state such as is the case for the shell or membrane element formulations available in ABAQUS, the strain component normal to the element in-plane directions (x, y), ε_{zz}, is not defined by the kinematics but by the restriction $\sigma_{zz} = 0$. Thus, the elastic prediction is carried from the Hooke's law, Eq. (2), written in the plane-stress state :

$$\sigma_{xx}^{trial} = \sigma_{xx}^{t} + \frac{E}{(1-\nu^2)}\left[\Delta\varepsilon_{xx} + \nu\,\Delta\varepsilon_{yy}\right] \tag{26}$$

$$\sigma_{yy}^{trial} = \sigma_{yy}^{t} + \frac{E}{(1-\nu^2)}\left[\Delta\varepsilon_{yy} + \nu\,\Delta\varepsilon_{xx}\right] \tag{27}$$

$$\sigma_{xy}^{trial} = \sigma_{xy}^{t} + \mu\,\Delta\gamma_{xy} \tag{28}$$

where E and ν are the Young modulus and the Poisson's ratio respectively. It should be noted that the shear strain components in ABAQUS are taken as $\gamma_{ij} = 2\varepsilon_{ij} (i \neq j)$. The plane-stress components $(\sigma_{xx}, \sigma_{yy}, \sigma_{xy})$ at the end of the time step for the UMAT and VUMAT subroutines are given respectively by :

$$\sigma_{xx}\Big|_{N} = \sigma_{xx}\Big|_{N-1} - \frac{E}{(1-\nu^2)}\left[c(\Delta\varepsilon_{xx}^{p}) + \nu\,c(\Delta\varepsilon_{yy}^{p})\right]_{N} \quad \text{and} \quad \sigma_{xx}^{t+\Delta t} = \sigma_{xx}^{trial} - \frac{E\,\Delta\overline{\varepsilon}^{p}}{(1-\nu^2)}\left[F_{,xx}^{trial} + \nu\,F_{,yy}^{trial}\right] \tag{29}$$

$$\sigma_{yy}\Big|_{N} = \sigma_{yy}\Big|_{N-1} - \frac{E}{(1-\nu^2)}\left[c(\Delta\varepsilon_{yy}^{p}) + \nu\,c(\Delta\varepsilon_{xx}^{p})\right]_{N} \quad \text{and} \quad \sigma_{yy}^{t+\Delta t} = \sigma_{yy}^{trial} - \frac{E\,\Delta\overline{\varepsilon}^{p}}{(1-\nu^2)}\left[F_{,yy}^{trial} + \nu\,F_{,xx}^{trial}\right] \tag{30}$$

$$\sigma_{xy}\Big|_{N} = \sigma_{xy}\Big|_{N-1} - \mu\,c(\Delta\gamma_{xy}^{p})\Big|_{N} \quad \text{and} \quad \sigma_{xy}^{t+\Delta t} = \sigma_{xy}^{trial} - \mu\,\Delta\overline{\varepsilon}^{p}\,F_{,xy}^{trial} \tag{31}$$

where the effective plastic strain increment for the VUMAT case, Eq. (25), is defined as :

$$\Delta\overline{\varepsilon}^{p} = \frac{F(\sigma_{ij}^{trial}) - \overline{\sigma}^{\,t}}{H(\overline{\sigma})^{t} + \dfrac{E}{(1-\nu^2)}\left[F_{,xx}^{trial}\,F_{,xx}^{trial} + F_{,yy}^{trial}\,F_{,yy}^{trial} + 2\nu F_{,xx}^{trial}\,F_{,yy}^{trial}\right] + \mu\,F_{,xy}^{trial}\,F_{,xy}^{trial}} \tag{32}$$

The increment of the total strain in the normal direction can be obtained from the additive strain decomposition, Eq. (1), that is, $\Delta\varepsilon_{zz} = \Delta\varepsilon_{zz}^{e} + \Delta\varepsilon_{zz}^{p}$, where :

$$\Delta\varepsilon_{zz}^{e} = -\frac{\nu}{E}\left[(\sigma_{xx}^{t+\Delta t} - \sigma_{xx}^{t}) + (\sigma_{yy}^{t+\Delta t} - \sigma_{yy}^{t})\right] \tag{33}$$

$$\Delta\varepsilon_{zz}^{p} = -(\Delta\varepsilon_{xx}^{p} + \Delta\varepsilon_{yy}^{p}) = -\Delta\overline{\varepsilon}^{p}\,(F_{,xx}^{trial} + F_{,yy}^{trial}) \tag{34}$$

and the corresponding total strain at the time of the end step is then updated as $\varepsilon_{zz}^{t+\Delta t} = \varepsilon_{zz}^{t} + \Delta\varepsilon_{zz}$.

2.3. Finite strain formulation

When the ∗ORIENTATION option in ABAQUS is used, the stress increments $\Delta\sigma_{ij}$ and the strain increments $\Delta\varepsilon_{ij}$ are expressed in the co-rotational frame $\mathbf{e_i}$ (ABAQUS, 2004). Therefore, the constitutive equations between stress and strain-rates are given in this frame by the strain-rate decomposition, Eq. (1), $\mathbf{D} = \mathbf{D^e} + \mathbf{D^p}$, the hypoelastic law, Eq. (2), $\dot{\sigma} = \mathbf{C^e} : \mathbf{D^e}$ and the associated flow rule, Eq. (3), $\mathbf{D^p} = \dot{\bar{\varepsilon}}^p F_{,ij}\, \mathbf{e_i} \otimes \mathbf{e_j}$ where the orthotropy axes are assumed to rotate with the co-rotational frame according to the spin rate.

2.4. Ferron's plasticity model

Ferron's plasticity model is based upon a parametric polar-coordinate description for orthotropic metal sheets under plane-stress conditions, *i.e.*, (σ_{xx},σ_{yy},σ_{xy}), used together with the assumption of isotropic hardening. This description is illustrated in Fig. 1, where the yield loci are defined in the principal stress space (σ_1,σ_2) and depend on the orientation between the principal stress axes (1,2) and in-plane orthotropy directions (*x*, *y*), *i.e.*, the angle α = (*x*,1) = (*y*, 2). The yield loci are normalized by the effective stress $\bar{\sigma}$ which is chosen as the equibiaxial yield stress σ_b and $g(\theta,\alpha)$ is the normalized radius defining a point on the yield locus whereas the polar angle θ defines the current stress state.

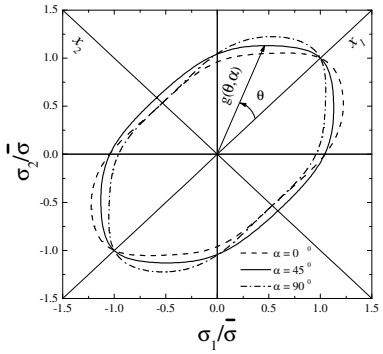

Figure 1. Ferron's plasticity model in the principal stress space (σ_1,σ_2) normalized by the effective stress $\bar{\sigma}$.

According to the assumption of isotropic work-hardening, the yield function can then be expressed as :

$$f = \phi(\sigma_1, \sigma_2, \alpha) - \bar{\sigma} \tag{35}$$

or, likewise, making the change of variables given by $x_1 = (\sigma_1 + \sigma_2)/2$ and $x_2 = (\sigma_1 - \sigma_2)/2$, as :

$$f = \psi(x_1, x_2, \alpha) - \bar{\sigma} \tag{36}$$

The function $g(\theta,\alpha)$ proposed by Ferron et al. (1994) is defined as :

$$(1-k)^{m/6}\, g(\theta,\alpha)^{-m} = F(\theta)^{m/6} - 2a \sin\theta \cos^{2n-1}\theta \cos 2\alpha + b \sin^{2p}\theta \cos^{2q} 2\alpha \tag{37}$$

where

$$F(\theta) = (\cos^2\theta + A\sin^2\theta)^3 - k\cos^2\theta(\cos^2\theta - B\sin^2\theta)^2 \tag{38}$$

In Eq. (37) the exponents *m*, *n*, *p* and *q* are positive integers and *a* and *b* are dimensionless parameters describing the in-plane anisotropy. In Eq. (38) *A* and *B* are positive constants whereas a positive *k*-value accounts for a flattening of the yield surface near plane-strain tension/compression and pure shear stress states. The coefficients *A*, *B* and *k* are determined from the experimental values of (σ_b/σ_{45}), (σ_b/τ_0) and R_{45} where τ_0 is the shear yield stress along the sheet rolling direction (RD) whereas R_{45} is the uniaxial plastic-strain ratio at 45^0 with respect to the RD. The recommended values for the exponents in Eq. (37) are *m = 2*, *n = 1* or *2*, *p* = 1 or *2* and *q = 1* or *2*. Then, the parameters *a* and *b* can be obtained from the *R*-values obtained at 0^0 and 90^0 from the RD, method *R*, or from the uniaxial yield stresses (σ_0,σ_{45},σ_{90}), method σ, as detailed elsewhere (Moreira, 2002). In addition, Hill's quadratic model (Hill, 1948) can be obtained as a particular case of Ferron's description by setting in Eq. (37) *k = 0*, *m = 2* and *n = p = q = 1*.

The extension to the 3D case is done assuming first that plastic flow is independent of the hydrostatic pressure. The effect of the normal stress component σ_{zz} is thus accounted for replacing σ_{xx} and σ_{yy} in the plane stress description by ($\sigma_{xx} - \sigma_{zz}$) and ($\sigma_{yy} - \sigma_{zz}$) respectively. Next, the effect of through-thickness shear stress components (σ_{xz},σ_{yz}) is considered by means of quadratic terms. Finally, the proposed 3D version of Ferron's plasticity model can be cast as :

$$f = \Phi(x_1, x_2, \alpha, \sigma_{xz}, \sigma_{yz}) - \bar{\sigma} = \sqrt{\psi^2(x_1, x_2, \alpha) + \beta\sigma_{xz}^2 + \gamma\sigma_{yz}^2} - \bar{\sigma} \tag{39}$$

where $\beta = \gamma = 3$ in the same way as for the von Mises isotropic yield criterion whereas $\psi(x_1, x_2, \alpha)$ is the Ferron's yield function for the plane-stress case, see Eq. (36), which can be defined for the purpose of FEM implementation by :

$$\psi(x_1, x_2, \alpha) = \left\{ \left[\frac{(x_1^2 + Ax_2^2)^3 - k\, x_1^2 (x_1^2 - Bx_2^2)^2}{(1-k)} \right]^{m/6} - \frac{2a}{(1-k)^{m/6}} \frac{x_2\, x_1^{2n-1}}{(x_1^2 + x_2^2)^{n-m/2}} \cos 2\alpha + \frac{b}{(1-k)^{m/6}} \frac{x_2^{2p}}{(x_1^2 + x_2^2)^{p-m/2}} \cos^{2q} 2\alpha \right\}^{1/m} \tag{40}$$

On the other hand, the variables x_1, x_2 and α characterizing the state of stress are linked to the plane-stress components (σ_{xx},σ_{yy},σ_{xy}) by :

$$x_1 = \frac{(\sigma_1 + \sigma_2)}{2} = \frac{(\sigma_{xx} + \sigma_{yy})}{2} \text{ and } x_2 = \frac{(\sigma_1 - \sigma_2)}{2} = \left[\sqrt{(\sigma_{xx} - \sigma_{yy})^2 / 4 + \sigma_{xy}^2} \right] \text{sign}(\sigma_{xy}) \tag{41}$$

$$\text{tg}2\alpha = \frac{2\sigma_{xy}}{(\sigma_{xx} - \sigma_{yy})} \tag{42}$$

Then, the partial derivatives of the function f, Eq. (36), are obtained from the consistency condition $df = 0$, *i.e.* :

$$df = \frac{\partial \psi}{\partial x_1} dx_1 + \frac{\partial \psi}{\partial x_2} dx_2 + \frac{\partial \psi}{\partial \alpha} d\alpha - d\bar{\sigma} = 0 \tag{43}$$

by calculating dx_1, dx_2 and $d\alpha$ from Eqs. (41-43) as a function of $d\sigma_{xx}$, $d\sigma_{yy}$ and $d\sigma_{xy}$ and replacing in Eq. (43) :

$$\frac{1}{2}\left[\frac{\partial \psi}{\partial x_1} + \cos 2\alpha \frac{\partial \psi}{\partial x_2} - \frac{\sin 2\alpha}{2x_2} \frac{\partial \psi}{\partial \alpha} \right] d\sigma_{xx} + \frac{1}{2}\left[\frac{\partial \psi}{\partial x_1} - \cos 2\alpha \frac{\partial \psi}{\partial x_2} + \frac{\sin 2\alpha}{2x_2} \frac{\partial \psi}{\partial \alpha} \right] d\sigma_{yy} + \frac{1}{2}\left[2 \sin 2\alpha \frac{\partial \psi}{\partial x_2} + \frac{\cos 2\alpha}{x_2} \frac{\partial \psi}{\partial \alpha} \right] d\sigma_{xy} - d\bar{\sigma} = 0 \tag{44}$$

Thus, by identifying the above differential form with the one obtained from the yield function expressed by Eq. (4), $f = F(\sigma_{xx},\sigma_{yy},\sigma_{xy}) - \bar{\sigma}$, it is readily observed that the coefficients of $d\sigma_{xx}$, $d\sigma_{yy}$ and $d\sigma_{xy}$ in Eq. (44) represent the partial derivatives $F_{,xx}$, $F_{,yy}$ and $F_{,xy}$, respectively. Once the derivatives $F_{,ij}$ is known as a function of the variables x_1, x_2 and α, the definition of the partial derivatives of the form $F_{,ijkl}$, see Eq. (22) is straightforward. Furthermore, the corresponding derivatives for the 3D case, Eq. (39), can be obtained in the same way as for the plane-stress case.

3. Associated numerical simulations of sheet-metal forming tests

The numerical simulations have been done with the finite element codes ABAQUS/Standard and ABAQUS/Explicit along with the user material subroutines **UMAT** and **VUMAT** respectively. In all the simulations discussed hereafter, the effective plastic stress-strain law is defined by the Swift-Krupkwoski power law :

$$\bar{\sigma} = K(\varepsilon_0 + \bar{\varepsilon}^p)^N \tag{45}$$

where K, ε_0 and N are the strength coefficient, the pre-strain and the strain-hardening exponent respectively. In all cases, the elastic constants are taken equal to E = 200,000 MPa and ν = 0.3. Moreover, the contact between the blank and the tooling is described by the Coulomb friction law. The numerical simulations were performed with a HP-UX 9000/785 J5600 with 1.5 Gb RAM workstation.

3.1 Hemispherical punch stretching test

The geometry adopted in the simulations of the hemispherical punch stretching test, shown in Fig. 2, is the same as in the work of Knibloe and Wagoner (1989). For the normal anisotropy case and due to axial symmetry, the analysis is reduced to an axisymmetric model. The tools are represented using rigid surfaces whereas the blank is meshed by 50 axisymmetric shell elements with 5 thickness integration points, SAX1 (ABAQUS, 2004). It should be observed that the range of stress states in the hemispherical punch stretching varies from the equibiaxial stretching at the pole (r = 0) to plane-strain tension on the clamped edge (r = 59.2 mm). Therefore, the ratio between the major principal stress in plane-strain tension and the equibiaxial yield stress, $P = \sigma_{PS1}/\sigma_b$, is the appropriate material parameter controlling the strain distributions in the hemispherical punch stretching.

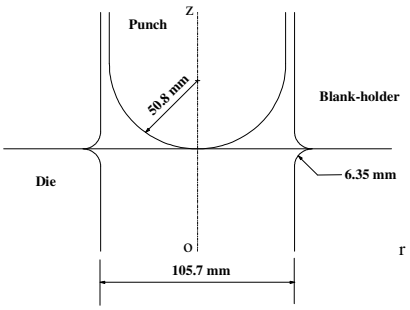

Figure 2. Schematic view of the hemispherical punch stretching test (Knibloe and Wagoner, 1989).

Figure 3 compares the experimental strains obtained by Knibloe and Wagoner (1989) for an aluminum killed steel tested under dry conditions and the predictions determined by Ferron's model with **UMAT**. The initial blank thickness is equal to 1.04 mm and its uniaxial hardening behavior is described by K = 598 MPa, N = 0.23 and ε_0 = 0.0023. The experimental value of the normal anisotropy coefficient R is 1.48. A good agreement for both hoop and radial strains is achieved with μ = 0.20 due to the small P-value (P = 1.099) obtained with Ferron's model. Actually, decreasing the ratio P favors the plastic flow under plane-strain stretching at the clamped edge in detriment to the radial displacement at the pole.

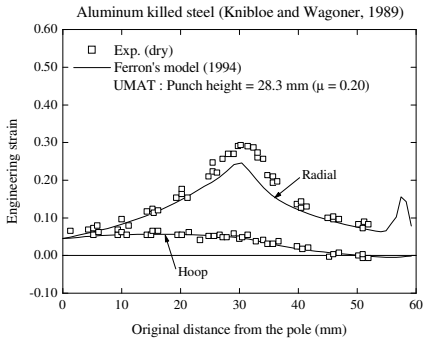

Figure 3. Numerical and experimental strain distributions obtained from the hemispherical punch stretching test.

3.2 Cup-drawing test

The geometry and the blank mesh used in the simulations of the cup-drawing test of an IF steel are shown in Fig. 4. Due to the material orthotropy and axial symmetry, only one quarter of the cup-drawing geometry is taken into account. The simulations were performed with the user subroutines **UMAT** and **VUMAT** as well as with Hill's quadratic model using the ABAQUS option *POTENTIAL. The tooling is represented by analytical rigid surfaces and 4 node rigid elements (R3D4) in ABAQUS/Standard and ABAQUS/Explicit FE codes respectively. The blank mesh is composed by 756 quadrangular reduced integration shell elements with five integration points through the thickness (S4R). The Coulomb friction coefficient has been taken equal to 0.15 between the punch and the blank and 0.05 elsewhere.

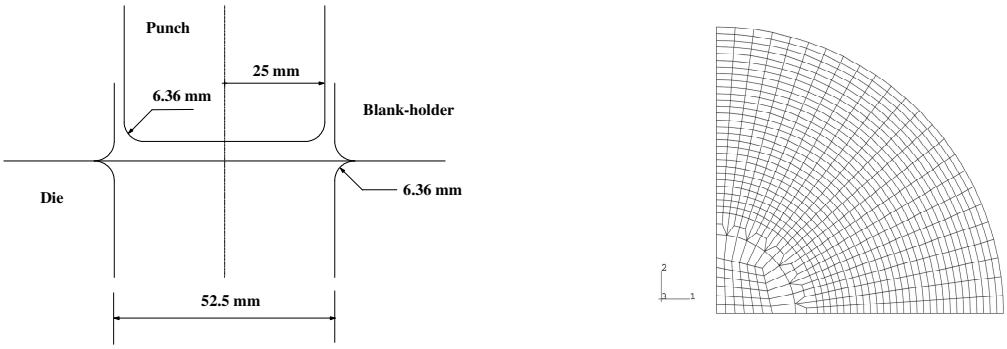

(a) (b)

Figure 4. Cup-drawing test numerical simulation : (a) tooling geometry and (b) finite element mesh of the blank.

Provided that only uniaxial tensile data was available, the coefficients of Ferron's model were determined by selecting first a positive *k*-value (0.2) and by imposing $B = 3A$. Then, A is calculated from the experimental R_{45} value. Fig. 5 compares the measured and predicted earing profiles as a function of the plasticity model and the method (R or σ) adopted to adjust the coefficients a and b describing the material anisotropy in Ferron's model. When these coefficients are fitted to the R-values the experimental height of ears at 0^0 and 90^0 is overestimated with Hill's quadratic model and underestimated with Ferron's model respectively. On the other hand, a better prediction is obtained when the material coefficients are adjusted to the σ-values. Finally, Tab. 1 compares the number of increments and the CPU time using the **UMAT** and **VUMAT** subroutine and the *POTENTIAL option in ABAQUS/Standard and Explicit respectively. Although the CPU times are larger, the use of Ferron's model leads to same order of increments obtained with the option *POTENTIAL, indicating a pertinent conditioning of the **UMAT** and **VUMAT** user subroutines.

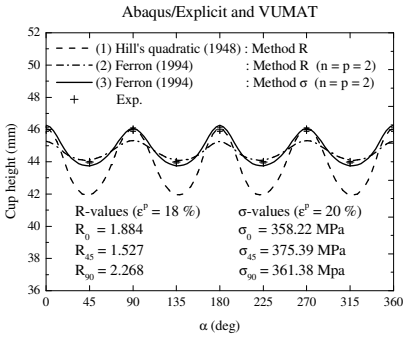

Figure 5. Experimental and predicted earing profiles obtained for an IF steel sheet (Moreira et al., 2000).

Table 1. Number of increments and CPU time obtained in the numerical simulation of the cup-drawing test.

	ABAQUS/Standard		ABAQUS/Explicit	
Plasticity model	Increments	CPU time (s)	Increments	CPU time (s)
Hill's quadratic	1373	10897	18207	582
Ferron	1317	16418	18607	859

4. Concluding remarks

In this work, the implementation procedures of Ferron's plasticity model in the ABAQUS FE codes together with the user subroutines **UMAT** and **VUMAT** were first detailed. Then, the predictions of sheet-metal forming tests, namely, the hemispherical punch stretching and the cup-drawing, have shown the consistency of either the predictions vis-à-vis the experimental data and the subroutines implementation procedures.

5. Acknowledgements

The authors would like to acknowledge ABAQUS Inc. for the research academic license of the ABAQUS FE codes. LPM is grateful to the research grants CNPq (476057/2003-5) and FAPERJ (E 26/170.566/2004).

6. References

ABAQUS, Version 6.4 Manuals, 2004, ABAQUS Inc., 1080 Main Street, Pawtucket, RI 02860-4847.

Ferron, G., Makkouk, R. and Morreale, J., 1994, "A Parametric Description of Orthotropic Plasticity in Metal Sheets", International Journal of Plasticity, Vol.10, pp. 51-63.

Hill, R. A, 1948, "Theory of the Yielding and Plastic Flow of Anisotropic Metals". Proceedings of the Royal Society of London, A 193, pp. 281-297.

Knibloe, J. R. and Wagoner, R. H., 1989, "Experimental Investigation and Finite Element Modeling of Hemispherically Stretched Steel Sheet", Metallurgical Transactions A, Vol. 20A, pp. 1509-1521.

Moreira, L. P., Ferron, G. and Ferran, G., 2000, "Experimental and Numerical Analysis of the Cup Drawing Test for Orthotropic Metal Sheets, Journal of Materials Processing Technology, Vol. 108, pp. 78-86.

Moreira, L. P., 2002, "Étude Numérique de l'Influence du Modèle de Plasticité sur le Comportement des Tôles lors de l'Emboutissage. Thèse de Doctorat, Université de Metz, Metz, France.

Simo, J. C. and Taylor, R. L., 1985, "Consistent Tangent Operators for Rate-Independent Elastoplasticity", Computer Methods in Applied Mechanics and Engineering, Vol. 48, pp. 101-118.

7. Responsibility notice

LPM and GF are the only responsible for the printed material included in this paper.